Predictions of nuclear β-decay half-lives with machine learning and their impact on r-process nucleosynthesis

Z. M. Niu (牛中明),[1,2] H. Z. Liang (梁豪兆),[3,4,*] B. H. Sun (孙保华),[5] W. H. Long (龙文辉),[6] and Y. F. Niu (牛一斐)[6,7]
[1]*School of Physics and Materials Science, Anhui University, Hefei 230601, China*
[2]*Institute of Physical Science and Information Technology, Anhui University, Hefei 230601, China*
[3]*RIKEN Nishina Center, Wako 351-0198, Japan*
[4]*Department of Physics, Graduate School of Science, The University of Tokyo, Tokyo 113-0033, Japan*
[5]*School of Physics and Nuclear Energy Engineering, Beihang University, Beijing 100191, China*
[6]*School of Nuclear Science and Technology, Lanzhou University, Lanzhou 730000, China*
[7]*ELI-NP, "Horia Hulubei" National Institute for Physics and Nuclear Engineering, RO-077125, Bucharest-Magurele, Romania*

(Received 2 October 2018; revised manuscript received 7 April 2019; published 5 June 2019)

Nuclear β decay is a key process to understand the origin of heavy elements in the universe, while the accuracy is far from satisfactory for the predictions of β-decay half-lives by nuclear models to date. In this work, we pave a novel way to accurately predict β-decay half-lives with the machine learning based on the Bayesian neural network, in which the known physics has been explicitly embedded, including the ones described by the Fermi theory of β decay, and the dependence of half-lives on pairing correlations and decay energies. The other potential physics, which is not clear or even missing in nuclear models nowadays, will be learned by the Bayesian neural network. The results well reproduce the experimental data with a very high accuracy and further provide reasonable uncertainty evaluations in half-life predictions. These accurate predictions for half-lives with uncertainties are essential for the r-process simulations.

DOI: 10.1103/PhysRevC.99.064307

I. INTRODUCTION

The origin of heavy elements, e.g., how and where the rare elements such as gold and platinum were created in the Universe, is a fascinating but still unanswered question of physics [1]. It relates to many branches of science, notably astrophysics and nuclear physics [2], so the answer to this question necessitates joint efforts of scientists from various fields. The rapid neutron-capture process (r process) is responsible for producing about half of the elements heavier than iron (Fe) and, in fact, the only mechanism for producing elements beyond Bi. However, the understanding of the r process still remains mysterious from the points of view of nuclear physics and astrophysics. Recent multimessenger observations including the gravitational-wave signal and multiwavelength electromagnetic counterparts strongly support the neutron-star merger to be a site of the production of heavy elements via the r process [3–5]. On the other hand, the measurements of nuclear properties also achieved great progress with the development of radioactive ion beam (RIB) facilities, especially the region around $N = 82$ [6–12]. These new observations and measurements make the r process a very hot topic in physics nowadays.

The r process which accounts for the origin of many heavy elements involves many unstable neutron-rich nuclei, namely the exotic ones. The experimental measurements are approaching the r-process paths around $N = 82$, while still far from ones around $N = 126$. Consequently, the reliable theoretical predictions of nuclear properties are necessary to the r-process simulations. Nuclear β decay is a decay process of a nucleus where it emits an electron and a neutrino, and hence it generates the new element with the proton number larger than parent nucleus. Therefore, nuclear β decay governs the abundance flow between neighboring isotopic chains in the r process and plays a key role in understanding the origin of heavy elements. However, the predictions of nuclear β-decay half-lives are rather difficult for nuclear theory due to the complexity in both interactions and nuclear many-body calculations. The accurate predictions of nuclear β-decay half-lives still remain an important but unsolved problem in nuclear physics. Theoretically, massive efforts have been devoted to this topic by developing the nuclear models based on various approximations or in a limited configuration space, such as gross theory (GT) [13–16], the quasiparticle random-phase approximation (QRPA) approach [17–27], and the shell model [28–32]. Unfortunately, the evaluations of theoretical uncertainties of β-decay half-lives are still very scarce in the literature, although they are essential to understand the reliability of theoretical predictions and further their impacts on the r process [33].

Machine learning, such as the pattern recognition and classification tasks, has been widely applied in engineering. It is very powerful in extracting pertinent features for complex nonlinear systems with complicated correlations, which are hard or even impossible to be tackled by traditional models. Therefore, it also provides a powerful tool in physics research, including particle physics [34–36] and condensed matter

*haozhao.liang@riken.jp

physics [37,38]. In nuclear physics, machine learning has been introduced to predict some nuclear properties based on the traditional neural network [39–43]. Comparing with conventional nuclear models, it constructs a neural network complex enough to predict nuclear properties accurately with many parameters, which in general accompanies with the overfitting problem and undetermined theoretical uncertainties. In contrast, machine learning with a Bayesian neural network (BNN) approach [44–48] can avoid overfitting automatically by including prior distribution and can quantify the uncertainties in its predictions naturally. Therefore, it is quite promising to predict nuclear β-decay half-lives accurately and give reasonable uncertainty evaluations with the BNN approach.

To better predict nuclear properties, it is important to include those well-known physics as much as possible before applying a BNN approach. Therefore, a more effective strategy is to use the BNN approach to improve the predictions of nuclear models. In this work, we will first propose a theoretical formula to predict nuclear β-decay half-lives based on the Fermi theory, and the BNN approach is then employed to improve the predictions of β-decay half-lives. The basic formulas of nuclear β-decay half-lives and BNN approach will be given in Sec. II. The results of β-decay half-lives and their impacts on solar r-process simulations will be discussed in Sec. III. Finally, a summary and perspectives will be presented in Sec. IV.

II. NUCLEAR β-DECAY HALF-LIVES AND BAYESIAN NEURAL NETWORK APPROACH

Let us start with the well-known Fermi theory of β decay [49], in which the nuclear β-decay half-life in the allowed Gamow-Teller approximation is predicted by

$$T_{1/2} = \frac{D}{g_A^2 \sum_{E_m<Q_\beta} B(E_m) f(Z,A,E_m)}, \tag{1}$$

where $D = 6163.4$ s and g_A is the effective weak axial nucleon coupling constant. $B(E_m)$ is the transition strength from the ground state of the parent nucleus to the excited state m of the daughter nucleus as a function of transition energy E_m. The total β-decay energy $Q_\beta = m_P - m_D - m_e$, where m_P, m_D, and m_e are the masses of parent nucleus, daughter nucleus, and electron, respectively. $f(Z,A,E_m)$ is the integrated lepton (e^-, $\bar{\nu}_e$) phase volume, where Coulomb screening and relativistic nuclear finite-size corrections have been considered [19].

When $E_m \gg m_e$, nuclear half-lives are mainly determined by $f(Z,A,E_m)$ since it is proportional to E_m^5. However, the accurate predictions of $B(E_m)$ are still very difficult for present nuclear models, which can only reproduce experimental half-lives within a few orders of magnitude. Therefore, we could approximatively predict nuclear half-life with

$$T_{1/2} = a/f(Z,A,E_m), \tag{2}$$

where E_m is estimated by $E_m = Q_\beta - b(1-\delta)/\sqrt{A}$ with $\delta = 1, 0, -1$ for even-even nuclei, odd A nuclei, and odd-odd nuclei, respectively. In this work, the Q_β are calculated using the mass predictions of WS4 model [50]. The parameters $a = 4.96$ and $b = 8.51$ are determined by the best fitting to experimental β-decay half-lives from NUBASE2016 [7], while only those nuclei with $Z, N \geqslant 8$, $T_{1/2} \leqslant 10^6$ s, and decaying 100% by the β^- mode are considered.

Since nuclear half-lives vary by many orders of magnitude, the root-mean-square (rms) deviation of logarithm of half-life $\log_{10}(T_{1/2})$ is usually employed to evaluate the accuracy of nuclear models

$$\sigma_{\rm rms}(\log_{10} T_{1/2}) = \sqrt{\frac{\sum_{i=1}^{n}\left[\log_{10}\left(T_{1/2}^{\rm exp}/T_{1/2}^{\rm th}\right)\right]_i^2}{n}}, \tag{3}$$

where $T_{1/2}^{\rm exp}$ and $T_{1/2}^{\rm th}$ are the experimental and theoretical half-lives, respectively, and n is the number of nuclei in a given evaluation set. In this work, the experimental data are taken from NUBASE2016, in which only those nuclei with $Z, N \geqslant 8$, $T_{1/2} \leqslant 10^6$ s, and decaying 100% by the β^- mode are considered. It is surprising that this "oversimplified" formula can already reproduce the known half-lives with $\sigma_{\rm rms}(\log_{10} T_{1/2}) = 0.81$, although it cannot account for the distribution of the Gamow-Teller strengths and possible impact of the first-forbidden transitions. This accuracy is even similar to that obtained by the sophisticated QRPA model based on the finite-range droplet model (FRDM) [23], whose $\sigma_{\rm rms}(\log_{10} T_{1/2})$ is 0.82. Similar empirical formulas had been used in the early estimates of β-decay half-lives used for the canonical r-process studies [51]. Taking Ni isotopes as typical examples, it is shown in Fig. 2 that Eq. (2) generally reproduces the data within less than one order of magnitude of accuracy, while showing systematic overestimation of nuclear β-decay half-lives with too-strong odd-even staggering. Such discrepancies from the data, which account for the physics missing in nuclear models, will be dealt with using the BNN approach in this work.

In the Bayesian approach, the model parameters $\boldsymbol{\omega}$ are described probabilistically while they are not fixed values as in our traditional view. Suppose we have a set of data $D = \{(\boldsymbol{x_1}, t_1), (\boldsymbol{x_2}, t_2), \ldots, (\boldsymbol{x_n}, t_n)\}$, where $\boldsymbol{x_k}$ and t_k ($k = 1, 2, \ldots, n$) are input and output data and n is the number of data. Then the probability distribution of $\boldsymbol{\omega}$ after the data D are taken into account, the posterior distribution $p(\boldsymbol{\omega}|D)$, is given based on Bayes's theorem,

$$p(\boldsymbol{\omega}|D) = \frac{p(D|\boldsymbol{\omega})p(\boldsymbol{\omega})}{p(D)} \propto p(D|\boldsymbol{\omega})p(\boldsymbol{\omega}), \tag{4}$$

where $p(\boldsymbol{\omega})$ is prior distribution based on our background knowledge, $p(D|\boldsymbol{\omega})$ is the likelihood function, and $p(D)$ is a normalization constant, which ensures the posterior distribution is a valid probability density and integrates to 1.

In this work, the prior distributions $p(\boldsymbol{\omega})$ are set as Gaussian distributions with zero means. The precisions (inverse of variances) of these Gaussian distributions are set as gamma distributions as in Ref. [47], which can make the precisions vary over a large range and the optimal values of precisions are then automatically found during the sampling process. The likelihood function $p(D|\boldsymbol{\omega})$ usually employ a Gaussian distribution, $p(D|\boldsymbol{\omega}) = \exp(\chi^2/2)$, where

$$\chi^2 = \sum_{n=1}^{N}\left[\frac{S(\boldsymbol{x};\boldsymbol{\omega}) - t_n}{\Delta t_n}\right]^2. \tag{5}$$

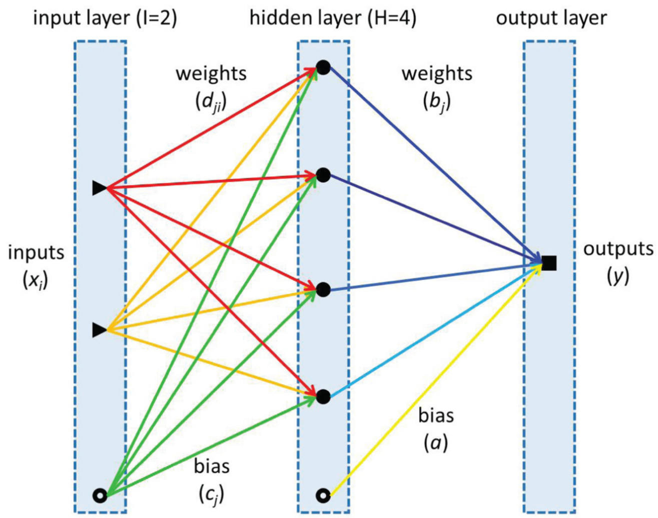

FIG. 1. A schematic diagram for a neural network with a single hidden layer, four neurons ($H = 4$), and two input variables ($I = 2$).

Here Δt_n is the associated noise error, and the inverse of its square $1/\Delta t_n^2$ is set to a gamma distribution as in Ref. [47]. The function $S(\boldsymbol{x};\boldsymbol{\omega})$ in the BNN approach is a neural network, i.e.,

$$S(\boldsymbol{x};\boldsymbol{\omega}) = a + \sum_{j=1}^{H} b_j \tanh\left(c_j + \sum_{i=1}^{I} d_{ji} x_i\right), \tag{6}$$

where $\boldsymbol{x} = \{x_i\}$ and $\boldsymbol{\omega} = \{a, b_j, c_j, d_{ji}\}$. H and I are the number of neurons in the hidden layer and the number of input variables, respectively. A schematic diagram for a neural network with a single hidden layer, four neurons ($H = 4$), and two input variables ($I = 2$) is shown in Fig. 1.

After specifying the the prior distribution $p(\boldsymbol{\omega})$ and likelihood function $p(D|\boldsymbol{\omega})$, the posterior distribution $p(D|\boldsymbol{\omega})$ can then be obtained by sampling using the Markov chain Monte Carlo algorithm. With the posterior distribution $p(D|\boldsymbol{\omega})$, the BNN prediction can be calculated by

$$\langle S \rangle = \int S(\boldsymbol{x};\boldsymbol{\omega}) p(D|\boldsymbol{\omega}) d\boldsymbol{\omega}, \tag{7}$$

whose uncertainty is estimated using $\Delta S = \sqrt{\langle S^2 \rangle - \langle S \rangle^2}$.

In this work, the BNN approach is employed to reconstruct residuals between $\log_{10}(T_{1/2}^{\rm exp})$ and $\log(T_{1/2}^{\rm th})$, i.e.,

$$t_k = \log_{10}\left(T_{1/2}^{\rm exp}\right) - \log\left(T_{1/2}^{\rm th}\right) = \log_{10}\left(T_{1/2}^{\rm exp}/T_{1/2}^{\rm th}\right). \tag{8}$$

The half-life predictions with BNN approaches are then as

$$T_{1/2}^{\rm BNN} = T_{1/2}^{\rm th} \times 10^{S(\boldsymbol{x};\boldsymbol{\omega})}, \tag{9}$$

where $T_{1/2}^{\rm th}$ are calculated with Eq. (2) in the work. Since the β-decay half-lives are sensitive to the pairing effects and the decay energies, we further introduce δ and Q_β as the inputs of neural network apart from Z and N, i.e., $\boldsymbol{x} = (Z, N, \delta, Q_\beta)$. For comparison, another neural network with $\boldsymbol{x} = (Z, N)$ is also constructed. For simplicity, we will use BNN-I2 and BNN-I4 to denote the BNN approaches with $\boldsymbol{x} = (Z, N)$ and $\boldsymbol{x} = (Z, N, \delta, Q_\beta)$, respectively. Their numbers of neurons are taken as $H = 30$ and $H = 20$, respectively. As mentioned above, the experimental data are taken from NUBASE2016 [7] for those nuclei with $Z, N \geqslant 8$, $T_{1/2} \leqslant 10^6$ s, and decaying 100% by the β^- mode. There are 1009 data that compose the entire data set. We further separate the entire set into two different sets: the learning set and the validation set. The learning set is built by randomly selecting 900 nuclei from the entire set and the remaining 109 nuclei compose the validation set.

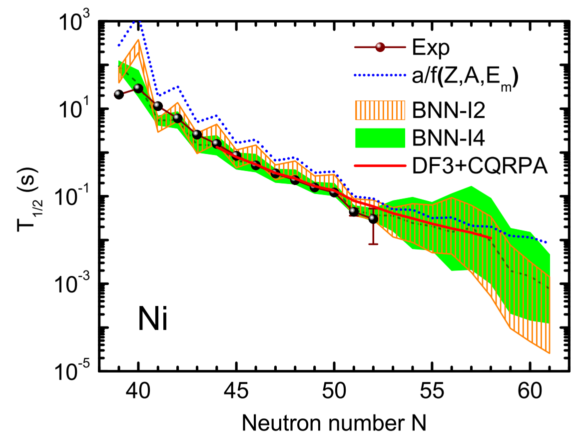

FIG. 2. β-decay half-lives of Ni isotopes. The experimental values in NUBASE2016 are denoted by spheres. The half-life predictions with Eq. (2) are shown by the dotted line, and their counterparts improved by BNN-I2 and BNN-I4 approaches and their uncertainties are shown by vertical line hatched region and green hatched region, respectively. The mean predicted half-lives of the BNN-I4 approach are marked by the dashed line. For comparison, the half-life predictions of the DF3 + CQRPA model are shown by the solid line.

III. RESULTS AND DISCUSSION

Figure 2 shows the predictions of BNN-I2 and BNN-I4 approaches for Ni isotopes, in comparison with the ones given by Eq. (2) and the data. It is found that the BNN-I2 approach can eliminate the systematic overestimation of half-lives in the predictions of Eq. (2), while its odd-even staggering still remains. Implemented with the BNN-I4 approach, this odd-even staggering is removed to a large extent and the resulting predictions are in excellent agreement with the experimental data. For comparison, the half-life predictions of the density functional of Fayans (DF3) + continuum QRPA (CQRPA) model [27] are shown by the solid line. The DF3 +CQRPA model well reproduces the known half-lives of Ni isotopes with $N \leqslant 50$ and slightly overestimates the known half-lives of ^{79,80}Ni. For Ni isotopes with $N > 52$, the half-life predictions of DF3 + CQRPA agree well with the mean predicted values of BNN-I4 approach. This may indicate that the BNN approach, including some known physics, paves an effective way for the reliable and accurate prediction of the nuclear β-decay half-life. In the following, therefore, we will only show our results based on the BNN-I4 approach.

As further illustration, taking $N = 82$ as examples, Fig. 3 shows the comparison between the predictions of BNN-I4 approach and other successful theoretical models, including

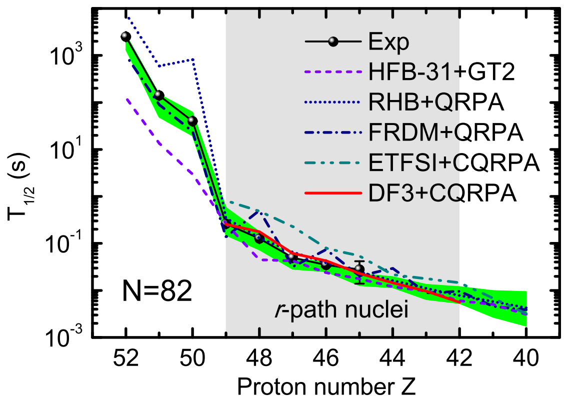

FIG. 3. β-Decay half-lives of Ni isotopes and $N = 82$ isotones. The predictions of the BNN-I4 approach are shown by the green hatched regions. The experimental values in NUBASE2016 are denoted by spheres. For comparison, the theoretical results from the HFB-31 + GT2, RHB + QRPA, FRDM + RPA, ETFSI + CQRPA, and DF3 + CQRPA models are shown by the dashed, dotted, dash-dotted, dash-dot-dotted, and solid lines, respectively.

the Hartree-Fock-Bogoliubov (HFB-31) + GT2 [14], relativistic Hatree-Bogoliubov (RHB) + QRPA [24], FRDM + QRPA [23], extended Thomas-Fermi plus Strutinsky integral (ETFSI) + CQRPA [25], and DF3 + CQRPA [26] models. Once again, the results of the BNN-I4 approach are in good agreement with the experimental data and even completely agree with the experimental data within uncertainties. On the contrary, the results from other theoretical models usually show some deviations from the experimental data. For example, the HFB-31 + GT2 model generally underestimates the known half-lives, the RHB + QRPA model overestimates the known half-lives when $Z \geqslant 50$, the FRDM + QRPA model shows strong odd-even staggering when $43 \leqslant N \leqslant 49$, and the ETFSI + CQRPA model slightly overestimates the known half-lives. However, the DF3 + CQRPA model well reproduces the known half-lives. When extrapolated to the unknown region, the uncertainties of BNN-I4 predictions increase slightly for $N = 82$ isotones, and the predictions of other theoretical models generally agree with the BNN-I4 predictions within uncertainties. Notice that the uncertainties of BNN-I4 predictions increase remarkably for Ni isotopes when extrapolated to the unknown region (see Fig. 2). It is interesting to notice that the BNN-I4 half-life predictions of Ni isotopes slowly decrease in the region $N = 51$–58 and suddenly drop at $N = 59$. This phenomenon may originate from the microscopic shell effect, since the last-occupied single-neutron orbitals are all $1g_{7/2}$ for nuclei $^{79-86}$Ni as indicated by the calculations with the mean-field model. Since the uncertainties of the BNN predictions in this region are large, future measurements on the half-lives of Ni isotopes are necessary to confirm whether this phenomenon is real.

In order to evaluate the global reliability of BNN approach to predict nuclear β-decay half-lives, the rms deviations $\sigma_{\rm rms}(\log_{10} T_{1/2})$ of BNN-I4 predictions with respect to the experimental data from the learning set and the validation set are presented in Figs. 4(a) and 4(b), respectively. For comparison, the corresponding results based on RHB + QRPA, FRDM + QRPA, and Eq. (2) are shown as well. It can be clearly seen that the theoretical approaches in general better reproduce the experimental data of nuclei with shorter half-lives. The BNN-I4 approach significantly improves the half-life predictions of Eq. (2) with much better accuracy than the selected models not only for the learning set but also for the validation set. It is worthwhile to mention that the nuclei along or near the r-process path are in general characterized by the typical half-lives less than 1 s. For these nuclei, which are in particular our focus, the $\sigma_{\rm rms}(\log_{10} T_{1/2})$ of BNN-I4 approach is only about 0.2. Namely the BNN-I4 approach can describe these relevant nuclear half-lives within a factor of two with respect to the experimental data ($10^{0.2} = 1.6$). Such high accuracy, which is achieved for the first time, is essential for the r-process simulations.

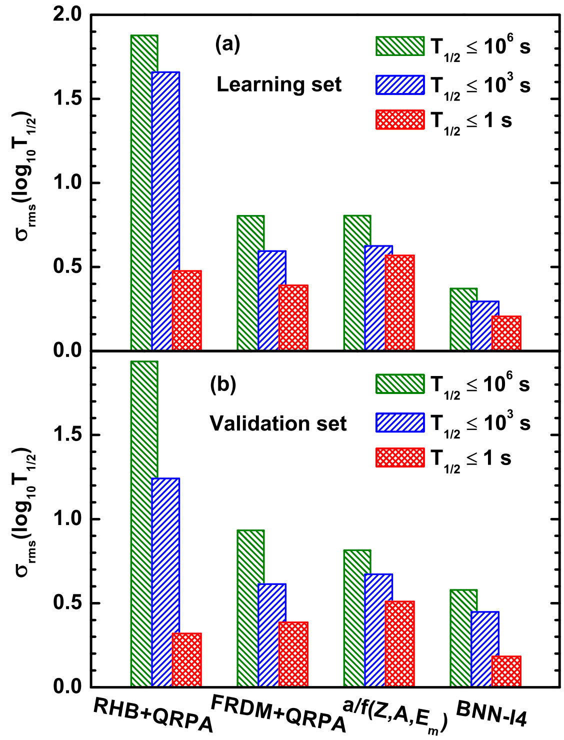

FIG. 4. The rms deviations $\sigma_{\rm rms}(\log_{10} T_{1/2})$ with respect to the known β-decay half-lives from the learning set (a) and the validation set (b). In each panel, three sets of nuclei with $T_{1/2} \leqslant 10^6$ s, $T_{1/2} \leqslant 10^3$ s, and $T_{1/2} \leqslant 1$ s are used in the rms evaluations.

Furthermore, with the present Bayesian scheme, it is natural to ask, "In case a few more nuclear half-lives are determined toward the neutron-drip line, how can these new data affect the predictions?" This is in particular an interesting question, since it is foreseen that even with next-generation RIB facilities it is still not feasible to reach all the r-process-path nuclei experimentally. Here let us assume that three more new β-decay half-lives were measured toward the neutron-drip line for each isotope, which are taken as the new experimental data in the BNN-I4 prediction. By further including these new artificial data to the learning set, the BNN-I4 approach is trained again. The resulting predictions are shown in Fig. 5 by taking $N = 126$ isotones as examples,

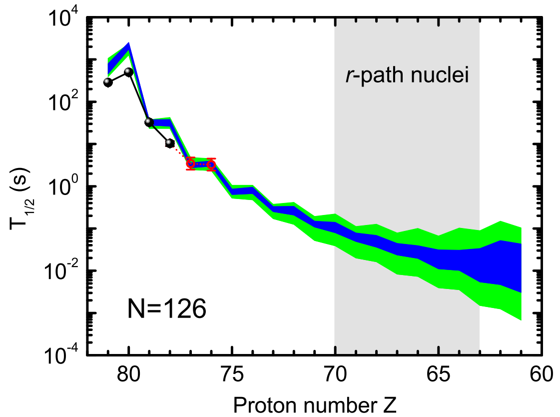

FIG. 5. β-Decay half-lives of $N = 126$ isotones. The green hatched region shows the predictions of BNN-I4 approach, whose learning data are only taken from NUBASE2016. The blue hatched region shows results of BNN-I4 approach as well, while its learning data are extended to include three extra β-decay half-lives for each isotope (denoted by open circles) toward the neutron-drip line. The experimental values in NUBASE2016 are denoted by spheres.

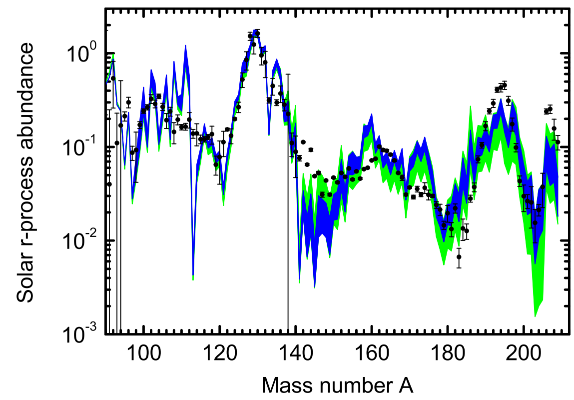

FIG. 6. Impact of nuclear β-decay half-lives on solar r-process calculations. The uncertainties bands for solar r-process abundances are due to the uncertainties of nuclear β-decay half-lives. The green and blue bands, respectively, correspond to the calculations using BNN-I4 half-life predictions, whose learning data are whether to include three new artificial β-decay half-lives for each isotope or not. The solar r-process abundances [52] are denoted by filled circles.

in which the original BNN-I4 results with learning data only from NUBASE2016 are denoted with the green hatched region and the blue one corresponds to the BNN-I4 results with three more artificial learning data. As expected, in the known region, even if the new artificial data are included, the uncertainties of BNN-I4 predictions remain almost the same as before. However, when extending the unknown region, the new artificial data make the uncertainties decrease by about a factor of 3. It is very important to the r-process studies. Although many r-process-path nuclei around $N = 126$ are still hard to measure even in the new-generation RIB facilities, this fact tells us the uncertainties of half-life predictions can be significantly reduced with only a few more measured data toward the neutron-drip line for each isotope.

Nuclear β-decay governs the r-process abundance flow between neighboring isotopic chains, so the uncertainties in nuclear β-decay half-lives would affect the r-process abundance distributions [53]. Figure 6 presents the solar r-process calculations based on the classical r-process model [54–56]. In our calculations, the experimental data including nuclear masses [6] and β-decay half-lives [7] are used if available; otherwise, we employed the WS4 model to determine the unknown masses and the BNN-I4 approach for the half-lives. The uncertainties bands in Fig. 6 for the solar r-process abundances are due to the uncertainties of nuclear β-decay half-lives, which come from the experimental errors if available and otherwise come from the uncertainties estimated with BNN-I4 approach. The green and blue bands correspond to the results without and with three new artificial data for each isotope when training the BNN-I4 half-life predictions, respectively.

Notice that the measurements have approached the r-process path at $N = 82$, while they are still far from the ones around $N = 126$. As a result, the half-life uncertainties for r-process-path nuclei around $N = 82$ are much smaller than those for r-process-path nuclei around $N = 126$, see Figs. 3 and 5. Coincidentally, as shown Fig. 6, the uncertainties of solar r-process calculations at $A \gtrsim 140$ are significantly larger than those at $A \lesssim 140$. However, as indicated by the theoretical uncertainties with BNN-I4 approaches, it is quite expectable that the large uncertainties for the r-process abundances at $A \gtrsim 140$ can be remarkably reduced with several new data toward the neutron-drip line measured. It also indicates that future relevant experiments would significantly improve our understanding of the r process.

IV. SUMMARY AND PERSPECTIVES

In summary, the machine-learning approach based on the Bayesian neural network is employed to predict nuclear β-decay half-lives accurately and give reasonable uncertainty evaluations. To possess better predictive power, a theoretical formula for β-decay half-lives with only two parameters is proposed based on the Fermi theory, which can already reproduce the data in a similar precision as the sophisticated FRDM + QRPA model. Then the BNN approach is trained to improve the predictions of the proposed formula by simulating the missing physics. It is found that after including more physics features related to the pairing effects and the decay energies, the machine-learning approach can precisely describe the general evolution of half-lives along isotopic and isotonic chains, including the odd-even effects which are difficult to be described by the nuclear models. Relatively large uncertainties of the present BNN half-life predictions are observed when extrapolated to the unknown region. Future studies on the half-life predictions with different BNN structures are envisaged, and a more appropriate BNN structure may help to improve extrapolation ability of BNN approach. Collaborating with the predicted nuclear β-decay half-lives and theoretical uncertainties, the impact on the r-process abundance distributions is further investigated. It is found that that the uncertainties of β-decay half-lives have consistently large influence on the solar r-process calculations when $A \gtrsim 140$. Fortunately, as revealed by the BNN approaches, the large uncertainties can be remarkably reduced if a few more nuclear half-lives are further determined toward the neutron-drip line for each isotope. It also becomes quite expectable that future measurements on half-lives could substantially improve our understanding on the *r* process.

ACKNOWLEDGMENTS

We are grateful to Professor T. Hatsuda and Dr. K. Yoshida for the fruitful discussions. This work was partly supported by the National Natural Science Foundation of China under Grants No. 11875070, No. 11675065, and No. 11711540016; the Natural Science Foundation of Anhui Province under Grant No. 1708085QA10; the Open fund for Discipline Construction, Institute of Physical Science and Information Technology, Anhui University; the JSPS Grant-in-Aid for Early-Career Scientists under Grant No. 18K13549; the JSPS-NSFC Bilateral Program for Joint Research Project on Nuclear mass and life for unravelling mysteries of the *r* process; and the RIKEN iTHEMS program.

[1] E. Haseltine, Discover **23**, 37 (2002).
[2] E. Margaret Burbidge, G. R. Burbidge, W. A. Fowler, and F. Hoyle, Rev. Mod. Phys. **29**, 547 (1957).
[3] B. P. Abbott *et al.* (LIGO Scientific Collaboration and Virgo Collaboration), Phys. Rev. Lett. **119**, 161101 (2017).
[4] I. Arcavi *et al.*, Nature **551**, 64 (2017).
[5] E. Pian *et al.*, Nature **551**, 67 (2017).
[6] M. Wang, G. Audi, F. G. Kondev, W. J. Huang, S. Naimi, and Xing Xu, Chin. Phys. C **41**, 030003 (2017).
[7] G. Audi, F. G. Kondev, M. Wang, W. J. Huang, and S. Naimi, Chin. Phys. C **41**, 030001 (2017).
[8] B. Franzke, H. Geissel, and G. Münzenberg, Mass Spectrom. Rev. **27**, 428 (2008).
[9] B. H. Sun, Yu. A. Litvinov, I. Tanihata, and Y. H. Zhang, Front. Phys. **10**, 102102 (2015).
[10] S. Nishimura *et al.*, Phys. Rev. Lett. **106**, 052502 (2011).
[11] G. Lorusso *et al.*, Phys. Rev. Lett. **114**, 192501 (2015)
[12] J. Wu *et al.*, Phys. Rev. Lett. **118**, 072701 (2017)
[13] K. Takahashi and M. Yamada, Prog. Theo. Phys. **41**, 1470 (1969).
[14] T. Tachibana, M. Yamada, and Y. Yoshida, Prog. Theo. Phys. **84**, 641 (1990).
[15] H. Nakata, T. Tachibana, and M. Yamada, Nucl. Phys. A **625**, 521 (1997).
[16] H. Koura and S. Chiba, Phys. Rev. C **95**, 064304 (2017).
[17] J. Engel, M. Bender, J. Dobaczewski, W. Nazarewicz, and R. Surman, Phys. Rev. C **60**, 014302 (1999).
[18] F. Minato and C. L. Bai, Phys. Rev. Lett. **110**, 122501 (2013).
[19] Z. M. Niu, Y. F. Niu, H. Z. Liang, W. H. Long, T. Nikšić, D. Vretenar, and J. Meng, Phys. Lett. B **723**, 172 (2013).
[20] Z. M. Niu, Y. F. Niu, Q. Liu, H. Z. Liang, and J. Y. Guo, Phys. Rev. C **87**, 051303(R) (2013).
[21] Z. Y. Wang, Y. F. Niu, Z. M. Niu, and J. Y. Guo, J. Phys. G: Nucl. Part. Phys. **43**, 045108 (2016).
[22] Z. M. Niu, Y. F. Niu, H. Z. Liang, W. H. Long, and J. Meng, Phys. Rev. C **95**, 044301 (2017).
[23] P. Möller, B. Pfeiffer, and K.-L. Kratz, Phys. Rev. C **67**, 055802 (2003).
[24] T. Marketin, L. Huther, and G. Martínez-Pinedo, Phys. Rev. C **93**, 025805 (2016).
[25] I. N. Borzov and S. Goriely, Phys. Rev. C **62**, 035501 (2000).
[26] I. N. Borzov, Phys. Rev. C **67**, 025802 (2003).
[27] I. N. Borzov, Phys. Rev. C **71**, 065801 (2005).
[28] K. Langanke and G. Martínez-Pinedo, Rev. Mod. Phys. **75**, 819 (2003).
[29] G. Martínez-Pinedo and K. Langanke, Phys. Rev. Lett. **83**, 4502 (1999).
[30] J. J. Cuenca-García, G. Martínez-Pinedo, K. Langanke, F. Nowacki, and I. N. Borzov, Eur. Phys. J. A **34**, 99 (2007).
[31] T. Suzuki, T. Yoshida, T. Kajino, and T. Otsuka, Phys. Rev. C **85**, 015802 (2012).
[32] Q. Zhi, E. Caurier, J. J. Cuenca-García, K. Langanke, G. Martínez-Pinedo, and K. Sieja, Phys. Rev. C **87**, 025803 (2013).
[33] M. R. Mumpower, R. Surman, G. C. McLaughlin, and A. Aprahamian, Prog. Part. Nucl. Phys. **86**, 86 (2016).
[34] P. Baldi, P. Sadowski, and D. Whiteson, Nat. Commun. **5**, 4308 (2014).
[35] L. G. Pang, K. Zhou, N. Su, H. Petersen, H. Stöcker, and X. N. Wang, Nat. Commun. **9**, 210 (2018).
[36] J. Brehmer, K. Cranmer, G. Louppe, and J. Pavez, Phys. Rev. Lett. **121**, 111801 (2018).
[37] J. Carrasquilla and R. G. Melko, Nat. Phys. **13**, 431 (2017).
[38] G. Carleo and M. Troyer, Science **355**, 602 (2017).
[39] J. W. Clark, in *Scientific Applications of Neural Nets*, edited by J. W. Clark, T. Lindenau, and M. L. Ristig (Springer-Verlag, Berlin, 1999), p. 1.
[40] K. A. Gernoth, in *Scientific Applications of Neural Nets*, edited by J. W. Clark, T. Lindenau, and M. L. Ristig (Springer-Verlag, Berlin, 1999), p. 139.
[41] H. F. Zhang, L. H. Wang, J. P. Yin, P. H. Chen, and H. F. Zhang, J. Phys. G: Nucl. Part. Phys. **44**, 045110 (2017).
[42] N. J. Costiris, E. Mavrommatis, K. A. Gernoth, and J. W. Clark, Phys. Rev. C **80**, 044332 (2009).
[43] N. J. Costiris, E. Mavrommatis, K. A. Gernoth, and J. W. Clark, arXiv:1309.0540 [nucl-th].
[44] C. M. Bishop, *Pattern Recognition and Machine Learning* (Springer, Singapore, 2006).
[45] R. Neal, *Bayesian Learning of Neural Network* (Springer, New York, 1996).
[46] R. Utama, J. Piekarewicz, and H. B. Prosper, Phys. Rev. C **93**, 014311 (2016).
[47] Z. M. Niu and H. Z. Liang, Phys. Lett. B **778**, 48 (2018).
[48] Léo Neufcourt, Yuchen Cao, Witold Nazarewicz, and Frederi Viens, Phys. Rev. C **98**, 034318 (2018).
[49] E. Fermi, Z. Phys. **88**, 161 (1934).
[50] N. Wang, M. Liu, X. Z. Wu, and J. Meng, Phys. Lett. B **734**, 215 (2014).

[51] *Essays in Nuclear Astrophysics*, edited by C. A. Barnes, D. D. Clayton, and D. N. Schramm (Cambridge University Press, London, 1982)

[52] C. Sneden, J. J. Cowan, and R. Gallino, Annu. Rev. Astron. Astrophys. **46**, 241 (2008) and references therein.

[53] Z. Li, Z. M. Niu, and B. H. Sun, Sci. China-Phys. Mech. Astron. **62**, 982011 (2019).

[54] B. Pfeiffer, K.-L. Kratz, and F.-K. Thielemann, Z. Phys. A **357**, 235 (1997).

[55] B. Sun, F. Montes, L. S. Geng, H. Geissel, Yu. A. Litvinov, and J. Meng, Phys. Rev. C **78**, 025806 (2008).

[56] Z. M. Niu, B. Sun, and J. Meng, Phys. Rev. C **80**, 065806 (2009).